

## The Optical Fiber Fault Detection By Computer Simulation for OFDR System

Dr. Hussain Joma Abbas\* & Salah Al – Adnan Taha 

Received on: 11/8/2009

Accepted on:5/8/2010

### Abstract

Mathematical simulation and theoretical investigation for faults detection in optical fibers were discussed by using computer simulation. The purpose of this work is to detect the faults that lead to decrease the level of the signal of the single mode fiber (SMF) for a length of (20km) for two wavelengths (1310nm & 1550nm) with attenuation of (0.34dB/km & 0.2dB/km) respectively by using Optical Frequency Domain Reflectometer(OFDR).The fusion splice is assumed to be existent about (5km),the connector about (10km) and the bend about (15km). The losses of these splices, bends, connectors and the levels of the reflected signals from the beginning of the fiber to its end have been calculated for two wavelengths. The calculation of the reflected signals by OFDR system has shown high resolution. the attenuation of wavelength (1550) nm is less than (1310) nm especially in the long distances ( $Z \geq 15\text{km}$ ), where the bending leads to big attenuation for the wavelength (1550) nm than (1310) nm where the level of the reflected signals at the point of bending for wavelength (1550) nm was (-87.852dBm) and (-80.2dBm) for the wavelength (1310nm). A novel technique was used to detect the fault by (phase method) by using OFDR system, The degree of the phase is changing suddenly for the reflected signals in the places where the faults are happening. The phase degree increases with the increase of the fiber length.

### كشف عيوب الفايبر الضوئي بواسطة محاكاة الكومبيوتر لنظام الانعكاس الطيفي (OFDR)

#### أخلاصه

المحاكاة الرياضية والتحقيق النظري لكشف العيوب في الألياف الضوئية نوقشت باستعمال المحاكاة بالحاسوب. تهدف هذه الدراسة إلى كشف العيوب التي تؤدي إلى تقليل مستوى الإشارة داخل الألياف الضوئية أحادية النمط (SMF) بطول (20km) وباستعمال الطول الموجي (1310nm) و(1550nm) والذي لهما توهين بمقدار (0.34dB/km) و (0.2dB/km) على التوالي بواسطة طريقة الانعكاس الطيفي (OFDR). تناول هذا البحث افتراض وجود الرابطة المنصهر (Fusion Splice) على بعد (5km) من بداية الليف الضوئي والموصل (Connector) على بعد (10km) والانحناء (Bending) على بعد (15km). تم حساب الخسائر والإشارات المنعكسة في الروابط والموصلات والانحناءات وللطولين الموجيين المذكورين في أعلاه. إن استخراج الخسائر والإشارات المنعكسة بطريقة الكشف البصري الطيفي (OFDR) تتمتع بتميز عالي (High resolution)، وقد لوحظ إن التوهين في الطول الموجي (1550nm) أقل مما هو عليه في (1310nm) وخصوصاً في المسافات الطويلة ( $Z \geq 15\text{km}$ ) بينما الانحناءات تؤدي إلى توهين في الطول الموجي (1550nm) أكبر مما هي عليه في (1310nm) حيث كان مستوى الإشارة المنعكسة عند نقطة الانحناء في الطول الموجي (1550nm) هو (-87.852dBm) بينما (-80.2dBm) للطول الموجي (1310nm). تناول هذا البحث طريقة جديدة لكشف العيوب داخل الليف الضوئي وهي طريقة (الكشف الطوري) باستخدام نظام الكشف البصري الطيفي OFDR، إن درجة الطور للإشارات المنعكسة تتغير بسرعة في الأماكن التي تحدث فيها العيوب داخل الليف البصري، كما تبين إن درجة الطور تزداد بزيادة طول الليف البصري.

**Introduction**

The coherent optical frequency domain reflectometer (OFDR) technique is a critical diagnostic tool for light wave systems and components. It consists of analyzing the beat signal produced by the optical interference between a fixed reference reflection called local oscillator reflection and different reflections coming from the component under test. The interference signal is obtained with a Michelson interferometer for which the reflection at the end of one of the arms gives the reference signal, or local oscillator (LO)[1]. The device under test is connected to the other arm. Figure(1) presents the basic block diagram for OFDR measurements. The optical frequency of a laser source is swept linearly and the light is launched at the input arm of a Michelson interferometer. Because of the linearity of the optical frequency sweep, the beat frequency is proportional to the distance between the LO and the reflection point while the reflection intensity is given by the squared amplitude of the beat signal. The fusion splice is assumed to be existent about (5km), the connector about (10km) and the bend about (15km). The losses of these splices, bends, connectors and the levels of the reflected signals from the beginning of the fiber to its end have been calculated. A mathematical models of OFDR system were obtained to calculate the losses and reflected power of defected optical fiber.

**2.Coherence Range**

Since the signal is obtained from an interference between the device under test (DUT) and the LO, the range is limited by the coherence of the laser. If the distributed feedback laser (DFB) has a line width of about 1MHz over the whole tuning range, which gives a spatial range of about 80 m (depending on the strength of the reflections). Increasing the range is possible, but would require a tunable laser with smaller line width[1]. The coherence length ( $I_c$ ) is given by [2]:

$$I_c = \frac{c}{2 n_1 \Delta f} \dots\dots(1)$$

$\Delta f$  is the line width of the laser ,c is the light speed , $n_1$  is the refractive index of the SMF core[2]

**3. Sensitivity**

Due to the coherent detection (interference between a fixed LO and the reflection from the (DUT), the sensitivity is very high, above 100 dB in principle. However, strong reflections, even when they are from far away (i.e. further than the coherence length of the laser) generate a large background noise, which limits the sensitivity. The OFDR is thus better suited to the measurement of optical networks and devices with low back reflection levels, below -30 dB. This is not a major limitation anymore, since all recent systems have such a low back reflection[3].

**4. Spatial Resolution**

Spatial resolution is a key feature in reflectometry. For an ideal optical source with zero line width, the spacing between the fast Fourier transformer (FFT) frequencies gives the resolution limit[4] :

$$\Delta l = \frac{c}{2 n_1 \Delta u} \dots\dots(2)$$

$\Delta l$  is the Spatial Resolution,  $\Delta n$  is the total optical frequency sweep. The round-trip time of flight of the light in the test arm of the interferometer is given[4] :

$$t = 2 n_1 Z / C \dots\dots(3)$$

where Z is the distance of any point in the (DUT).The coherence time of the laser is given by [3] :

$$t_c = 1 / p . \Delta f \dots\dots(4)$$

Nonlinearities in the optical frequency sweep, will impose further limits on the resolution, because the beat frequency corresponding to a given reflection peak varies during the data acquisition. The nonlinearity arises because of the thermal response of the laser. Adding a second order term ( $\gamma$ ) to the optical frequency sweep the angular frequency of the light  $\omega(t)$  can be written as[4] :

$$W(t) = W_o + bt + gt^2 \dots(5)$$

where ( $\omega_o$ ) is the start frequency and ( $\beta$ ) is the sweep rate. Neglecting the laser phase noise, the optical beat signal  $I(t, \tau)$  corresponding to a single reflection in the test arm, at a distance ( $Z$ ) from the local oscillator will be given by[4] :

$$I(t, \tau) = (e^{-t/\tau_c}) \frac{E_o^2}{2} \sqrt{R_{LO} R_{DUT}} \cos\left[ \omega_o t - \frac{bt^2}{2} + \frac{gt^3}{3} + (bt - gt^2)t + gtt^2 \right] \dots(6)$$

$E_o^2$  is the laser optical power,  $R_{LO}$  is the reflectivities of the local oscillator,  $R_{DUT}$  is the reflectivities of single mode fiber (DUT). The beat frequency ( $f_b$ ) corresponding to this reflection will be given by[4].

$$2pf_b = (b - gt)t + 2ggt \dots(7)$$

which means that the beat frequency changes linearly along the sweep, no more being constant. In the case of a small nonlinearity ( $2\gamma t \ll \beta$ ) the reflection will be characterized by a peak in the frequency spectrum whose width is proportional to the round-trip time ( $\tau$ ), i.e., to the distance between the reflection and the local oscillator[4]. The sweep rate is given by[2]:

$$b = \frac{\Delta v}{\Delta T} \dots(8)$$

$\Delta T$  is the period of the triangular waveform. The beat frequency ( $f_b$ ) is given by[4][2]:

$$f_b = \frac{bt}{2p} \dots(9)$$

A full sweep of 6 GHz limiting the resolution to 1.6 cm. The choice of the full optical frequency span depends on the actual length of the device under test[2][4].

### 5. Losses of Fiber Optics

When several fibers are connected to form an installed cable plant, the optical time domain reflectometer (OTDR) and (OFDR) can characterize optical fiber and optical

connection properties along the entire length of the cable plant. A fiber optic cable plant consists of optical fiber cables, connectors, splices, mounting panels, jumper cables, and other components. A cable plant does not include active components such as optical transmitters or receivers. By analyzing the (OTDR and OFDR) plot, or trace, end users can measure fiber attenuation and transmission loss or (FAULTS) between any two points along the cable plant. End users can also measure insertion loss and reflectance of any optical connection. In addition, end users use the (OTDR and OFDR) trace to locate fiber breaks or (faults). A point defect, or fault, can be reflective or non reflective. A point defect normally exhibits a loss of optical power. However, Figure (2) shows different types of faults like fresnel reflection (initial input reflection), Splice fault ,connector fault (mechanical misalignment), or differences in the geometrical and waveguide characteristics of any two waveguides being joined ,bending fault, ending fresnel reflection fault. fresnel reflection indicating for starting and ending of optical fiber [5].

### 6. Fresnel Reflection

A major consideration with all types of fiber-fiber connection is the optical loss encountered at the interface. Even when the two jointed fiber ends are smooth and perpendicular to the fiber axes, and the two fiber axes are perfectly aligned, a small proportion of the light may be reflected back into the transmitting fiber causing attenuation at the joint. This phenomenon, known as Fresnel reflection, is associated with the step changes in refractive index at the jointed interface (i.e. glass-air-glass). The magnitude of this partial reflection of the light transmitted through the interface may be estimated using the classical Fresnel formula for light of normal incidence and is given by [6]

$$r = \left( \frac{n_1 - n}{n_1 + n} \right)^2 \dots(10)$$

Where  $r$  is the fraction of the light reflected at a single interface,  $n_1$  is the refractive index of the fiber core,  $n$  is the refractive index of the medium between the two jointed fibers (i.e. for air  $n=1$ ). The measure of the reflection properties of a fiber join is its return loss, defined by[7]:

$$a = -10 \log_{10} \left( \frac{P_{reflected}}{P_{incident}} \right) \dots\dots(11)$$

**7. Extrinsic Losses**

Single-mode fibers have core diameters on the order of 9µm. Owing to this microscopic size, mechanical misalignment is a major challenge in joining two fibers by connector or splice. Power losses result from misalignments because the radiation cone of the emitting fiber does not match the acceptance cone of the receiving fiber. The magnitude of the power loss depends on the degree of misalignment. Figure (3) illustrates one type of misalignment(Extrinsic) between two fibers.

**Axial displacement:**

Also called lateral displacement, results when the axes of the two fibers are offset by a distance ( $d$ ). The misalignment to which a connection is most sensitive is lateral displacement, shown in Figure(3). Mechanical misalignments of the fibers cause losses because of the areas of the fiber core do not overlap sufficiently. In the analysis of misalignments the usual assumptions are that the fibers have equal radii, index profiles, and numerical apertures to isolate the effects of the misalignment .The losses of lateral displacement misalignment for ( $d \ll \omega_0$ ) is[8].

$$L_{Lat}(dB) = -10 \log_{10} \left( \exp - \left( \frac{d}{\omega_0} \right)^2 \right) \dots\dots(12)$$

Where ( $\omega_0$ ) is the spot size of the fundamental mode. The spot size is

usually defined as the width to (1/e) intensity to the (LP<sub>01</sub>) mode, or in terms of the spot size of an incident Gaussian beam which gives maximum launching efficiency[6]. However, the spot size for the (LP<sub>01</sub>) mode (corresponding to HE mode) may be obtained from the empirical formula ( $\omega_0$ ) given by Marcuse [9][10].

$$\omega_0 = a \left( 0.65 + 1.619V^{-3/2} + 2.879V^{-1} \right) \dots\dots(13)$$

**8. Intrinsic Losses**

In addition to extrinsic misalignments, differences in the geometric and waveguide characteristics of any two mated fibers can have a profound effect on the joint loss. The differences include variations in core diameter, core-area ellipticity, numerical aperture, and core-cladding concentricity of each fiber. Since these are manufacturer-related variations, the user has little control over them, except to specify certain tolerances in these parameters when purchasing the fiber. For a given percentage mismatch between fiber parameters, differences in core sizes and numerical apertures have a significantly larger effect on joint losses than mismatches in the refractive-index profile or core ellipticity [11].

**Core area mismatches:** For simplicity let the subscripts E and R refer to the emitting and receiving fibers, respectively. If the axial numerical apertures and the core index profiles are equal that is ( $NA_E = NA_R$ ), ( $n_E = n_R$ ), but the fiber diameters ( $d_E$ ) and ( $d_R$ ) are not equal, then the coupling loss is[9]:

$$L_F(d) \begin{cases} -10 \log_{10} \left( \frac{d_R}{d_E} \right)^2 & \text{for } d_R < d_E \\ 0 & \text{for } d_R \geq d_E \end{cases} \dots\dots(14)$$

**9. Reflection from Connector Pair**

Figure (4) shows a model of an index-matched connection with perpen-

dicular fiber end faces. In this figure and in the following analyses, offsets and angular misalignments are not taken into account. The connection model shows that the fiber end faces have a thin surface layer of thickness ( $h$ ) having a high refractive index ( $n_2$ ) relative to the core index, which is a result of fiber polishing. The fiber core has an index ( $n_0$ ), and the gap width ( $d$ ) between the end faces is filled with index-matching material having a refractive index ( $n_1$ ). The return loss (RLIM) in decibels for the index-matched gap region is given by[9][12]:

$$RL_{im} = -10 \text{Log}_{10} \left\{ 2R \left[ 1 - \cos \left( \frac{4p \bar{n}_1 \bar{d}}{l} \right) \right] \right\} \dots(15)$$

**10. Bending Losses in Single Mode Fiber**

Bend losses are particularly important in single-mode fiber. In these fibers, the bend losses show a dramatic increase above a critical wavelength when the fiber is bent or perturbed. In particular, it has been observed that the bend losses can be appreciably high at 1550 nm than in fibers designed for operation at 1300 nm [13]. The susceptibility of a fiber to these losses depends on the mode-field diameter and the cutoff wavelength [9,14]. the worst-case condition is in a fiber with a large mode-field diameter and a low cut off wavelength, so bending losses are minimized in single-mode fibers by avoiding this combination of features[15]. There is essentially no bending loss until a certain critical radius is reached, whereupon the bending loss increases dramatically. Notice also that the critical bend radius is dramatically different for the two wavelengths. At 1310nm, the critical bend radius is about 1.5 cm; and the bending losses is (0.2) dB at bending radius of (1.35cm). At 1550nm the critical bend radius is about

2.5cm (these critical bend radius change, depending on the fiber’s numerical aperture and core radius) , so the bending loses is (8.3)dB at bending radius of(1.35)cm [8].

**11. Basic 2×2 Coupler**

The 2×2 coupler is a simple fundamental device that used here to demonstrate the operational principles of optical couplers. These are known as directional couplers. A common construction is the fused-fiber coupler illustrated in Figure (5). This is fabricated by twisting together, melting, and pulling two single-mode fibers so they get fused together over a uniform section of length W. Po is the input power on the top fiber (that takes as the primary fiber in a link), P1 is the throughput power, and P2 is the power coupled into the second fiber. Parameters P3 is extremely low optical signal levels below the input power level. These result from backward reflections and scattering due to packaging effects and bending in the device.

**12. Mathematical-Designing of faults detection model for the wavelengths 1310nm and 1550nm**

Simulink is a software package for modeling, simulating, and analyzing dynamical systems. It supports linear and nonlinear systems, modeled in continuous time, sampled time, or a hybrid of the two. Systems can also be multirate, i.e., have different parts that are sampled or updated at different rates. For modeling, Simulink provides a graphical user interface (GUI) for building models as block diagrams, using click-and-drag mouse operations. so anyone can build models using both top-down and bottom-up approaches. Simulink Matlab can view the system at a high level, then double-click on blocks to go down through the levels to see increasing levels of model detail. This approach provides insight into how a model is organized and how its parts interact[16]. Fault detection model was built by using OFDR system to detect any reflected signal along the single mode fiber SMF. Figure(6) was built to

detect all faults of optical fiber by using OFDR at wavelengths (1310 nm, 1550 nm) by (DFT-FFT), the faults are :

1. Fresnel reflection fault.
2. Splice fault.
3. Connector fault.
4. Bending fault

### 13. Results and Discussion

A summarized list for SMF parameters were given to the Table (1). The fraction of light ( $r$ ) reflected at a single interface (Fresnel reflection) was obtained from equation (10). For Fusion Splice the Lateral Displacement misalignment (round-trip) was calculated for wavelength 1310 nm and 1550 nm from equation (12) and equation (13). These parameters were given to the Table (2). For Connector the insertion losses (round-trip) or fault due to difference in core radius of two fibers was calculated from equation (14), where the numerical aperture and core index for emitting and receiving fiber are equal. The return losses from Connector pair were calculated from equation (15). All these parameters of Connector were summarized in the Tables (3) and (4). Insertion losses for the Bending for single mode fiber SMF was calculated, all parameters of Bending losses were given to the Table (5). A summarized list for Coupler Losses parameters were given to the Table (6). Scattering Coefficient ( $\alpha_s$ ) was 0.0615(1/km), 0.0313(1/km) for wavelengths 1310 nm and 1550 nm respectively [6]. The reflected power from oscillator was taken from equation (10). The distance from connector of oscillator source and coupler is 40 cm [9], see Table (7). The line-width of the source was tuned, so that the line-width of (5.14 kHz) was assumed [17]. The coherence range was calculated from equation (1). The total frequency linear sweep  $\Delta\nu$  of the laser source signal is (6 GHz) and its time  $T$  is (22 ms) considering the period of triangular waveform FFT triggering [4]. The spatial resolution  $\Delta l$  was taken from equation (2). The coherence time of the source was chosen from equation (4),

the linear sweep rate  $\beta$  of the laser source signal was taken from equation (8). All the above parameters were given to the Table (8) below. The losses ( $R_A$ ) due to Fresnel reflection and coupler losses at  $Z=0$  km taken from equation (10), Table (6) respectively were added to get total attenuation from the source until this point. Reflected power ( $R_A$ ) from (DUT) at this point was calculated from equation (11). The round trip-time of flight of light until this point was evaluated from equation (4). The linear beat frequency at this point in the (DUT) was taken from equation (9). The linear condition was taken in equation (6) and the non-linearity ( $\gamma$ ) becomes (zero) [4]. So, the coherence reflected power  $I_A(t, \tau)$  at this point was calculated from equation (6) under the above condition, and all the parameters were given in the Table (9) for wavelengths 1310 nm and 1550 nm. By the same method the coherence reflected power at  $Z = 0.96$  km, 5 km, 10 km, 15 km, and 20 km were calculated. A summarized list for these beat signals and their corresponding frequencies and distances values are given below in the Tables (10, 11) for wavelength 1310 nm and 1550 nm respectively, by using mathematical model (6) and table (10) fig. (7) show these relevant relations, by using mathematical model (6) and Table (11), fig. (8) show these relevant relations for 1310 nm and 1550 nm respectively. Figure (9, 10) show the relation between ( $\lambda_1$  and  $\lambda_2$ ). Fig. (7) shows OFDR signal trace of SMF with wavelength 1310 nm by using mathematical modeling of Simulink Matlab package fig. (6). The individual sharp spikes result from using FFT of different reflection faults. At  $Z=0$  one spike is appear results from Fresnel reflection with frequency of 0 MHz. At  $Z = 0.96$  km of fiber optic length, One sharp spike appears is resulted from the back reflection ( $I_B$ ) at beat frequency 0.4 MHz. At  $Z=5$  km, two sharp spikes are appeared at looking closely, the second spike ( $I_{C_2}$ ) is seen short after the first spike ( $I_{C_1}$ ) because the insertion losses of the splices is

(0.459)dB, table (2). At  $Z=10$ km, three sharp spikes are appeared, first spike ( $I_{D2}$ ) is resulted from reflection, second spike ( $I_{D1}$ ) is resulted from Fresnel reflection, third spike ( $I_{D3}$ ) is resulted from insertion losses of connector. At  $Z=15$ km, first sharp spike is resulted from reflection at this point with beat frequency 6.24MHz, Second spike is resulted from bending losses at this point (0.2)dB, table (5). At  $Z=20$ km, first spike ( $I_{F2}$ ) is resulted from reflection at this point, second large spike is resulted from Fresnel reflection at the end of fiber optic From fig.(9),(10), at short distances it appears that the reflected power at 1310nm is larger than that for 1550nm because the scattering coefficient ( $\alpha_s$ ) and backscattering factor (S) of 1310nm is larger than it in 1550nm, At long distances the reflected power at 1550nm become larger than it at 1310nm until the bending fault at distance 15km where the reflected power of the wavelength 1550nm become more attenuated than 1310nm, table(5). Phase method was built to detect the fault by using the phase of the reflected signals. Model of phase detection was built as illustrated in figure (6). The faults were assumed as in table (10,11). The reflected beat signal (magnitude Vs frequency) was shown in figure (11). The same reflected beat signal but between (phase Vs frequency, distance) was illustrated in figure (12),(13). Fig.(12),(13) shows the degree of phases for reflected signals are changed suddenly in the places where the faults are happening.

#### 14. Conclusions

OFDR systems and the related investigation by the fault of the SMF lead us to conclude the following: OFDR system has a better resolution than OTDR system. OFDR system is more sensitive than OTDR system in SMF[9]. At fusion splice point, the losses are the same at short/long wavelength. At bending point, the losses are more large for long wavelength. At connector point, the losses are the same at short / long wavelength. New technique of (phase detection) is used,

The degree of the phase is changing suddenly for the signals in the places where the faults are happening. The phase degree increases with the increase of the fiber length which means that this new method is very useful in the optical fiber and for very long distances.

#### 15. References

- [1] Huttner B. and Gisin "Optical Frequency Domain Reflectometry For characterization of optical Networks And Devices" Group of Applied Physics University of Geneva, 1999.
- [2] Yoshikot and Y. Sampei, "Optical Fiber Inspection Device" Yokogawa Electric Corporation, PP.1-14, Japan, 1999, USA patent documents.
- [3] Mussi G and Vonder Weid, "152.5dB sensitivity high dynamic range optical frequency domain reflectometry" Electronics Letter 32, pp.926, 1996.
- [4] Von der J. P., Weid, Rogiero Passy, and G.Mussi, "On the characterization of optical fiber network components with optical frequency domain reflectometry" J.Lightwave, vol.15, pp.113 1- 1141, Jul.1997
- [5] Kelley P. L. and Kaminon "Nonlinear Fiber Optics" Third Edition, Copyright by Academic Press, 2001.
- [6] John M. Senior "Optical Fiber Communications" Prentice-Hall, PP.69-154, 1985.
- [7] power J., "An Introduction To Fiber Optics Systems" McGraw-Hill, 1986.
- [8] Duwayne R. and Jonson "Troubleshooting Optical-Fiber Networks" Second Edition, Copyright, pp.21-33- 273, 2004.
- [9] Keiser Gerd, "Optical Fiber Communications", 3<sup>rd</sup> Edition, McGrawHill, PP.230-385, 2000.
- [10] Marcuse D. "Loss analysis of single-mode fiber splices", Tech.J.V.56, pp.703-718, Jun. 1977.
- [11] Abdullah A.Z. "Optical Communications Essentials" @ McGraw-Hill, 2004.
- [12] Kihara M. "Return loss characteristic of optical fiber

connectors", J. Lightwave Tech., Vol. 14, pp. 1986- 1991, Sep. 1996 .

[13] Kaiser P. and Keck" Fiber types and their status," pp.29-54, New York Academic Press, 1988.

[14] Artiglia M. "Simple and accurate microbending loss evaluation in generic single mode fibers," Proc. 12th ECOC, vol. 1, pp. 341-344, 1986.

[15] Charles H. "Optical fiber cables," pp. 217-261, New York: Academic Press, 1988.

[16] "Simulink Dynamic System Simulation for MATLAB", from Internet [www.mathworks.com](http://www.mathworks.com) by the Mathworks. Inc . 1999 .

[17] Francois J. and Allard" High-power and ultra narrow DFB Laser, The effect of Line width reduction systems on coherence length and interferometer noise" Spie, Vol.6216, May. 2006.

**Table (1) SMF calculations**

	$n_1$	$n_2$	NA	V	a ( $\mu\text{m}$ )	$\alpha$ (dB/km)
$\lambda_1 = 1310 \text{ nm}$	1.4524	1.4468	0.1274	2.404	4	0.34
$\lambda_2 = 1550 \text{ nm}$	1.4516	1.44402	0.1482	2.40	4	0.2

**Table (2) Insertion Losses for Splice (round-trip)**

	d ( $\mu\text{m}$ )	$\overline{W}_o$ ( $\mu\text{m}$ )	$L_{\text{Lat}}$ (dB)	r
$\lambda_1 = 1310 \text{ nm}$	1	4.35	0.459	0.034
$\lambda_2 = 1550 \text{ nm}$	1	4.4	0.466	0.034

Table (3) Insertion Losses of Connector

	$a_R$ (mm)	$a_E$ (mm)	$L_F(d)$ (dB)
$l_1 = 1310$ nm	3.0	4.0	5
$l_2 = 1550$ nm	3.0	4.0	5

Table (4) Return Losses From Connector

	$n_0 = n_1$	$r_1$	$r_2$	$n_1$	$n_2$	$\bar{d}$ (mm)	$h$ (mm)	$d$	$R$	$RL_{IM}(dB)$	$r_c = P_{ref}/P_{inc}$
$l_1 = 1310$ nm	1.4524	0.091	0.095	1	1.21	0.22	0.12	1.393	0.034	-43.3608	$4.612 \times 10^{-5}$
$l_2 = 1550$ nm	1.4516	0.091	0.095	1	1.21	0.22	0.12	1.1772	0.034	-44.822	$3.295 \times 10^{-5}$

Table (5) Bending Losses

	Critical Radius (cm)	Bending Radius (cm)	Losses (dB)
$l_1 = 1310$ nm	1.5	1.35	0.2
$l_2 = 1550$ nm	2.5	1.35	8.3

Table (6) Coupler Insertion Losses

	Excess Losses (dB)	Split Ratio	$P_o$ (mW)	$P_1=P_2$	Insertion Losses(dB)
$l_1 = 1310$ nm	0.2	50%	20	9.6 mW	6.2
$l_2 = 1550$ nm	0.2	50%	20	9.6 mW	6.2

Table (7) Reflected Oscillator Power (r.t.)

	$R_{Lo}$ (mW)	$L$ (cm)
$l_1 = 1310$ nm	0.157	40
$l_2 = 1550$ nm	0.157	40

Table (8) Characteristic of the Laser Source using in OFDR system

	Df (kHz)	$I_C$ (km)	$D\Omega$ (GHz)	$\Delta I$ (cm)	$t_c$ (ms)	DT (ms)	b(Hz/s)
$l_1 = 1310$ nm	5.14	20.09	6	1.72	61.93	22	$2.7 \times 10^{11}$
$l_2 = 1550$ nm	5.14	20.104	6	1.7	61.9	22	$2.7 \times 10^{11}$

Table (9) Reflected Power at Z = 0 km (r.t.)

	Z (km)	$t$ (ms)	r (dB)	$a_A$ (dB)	$R_A$ (mW)	$f_b$ (MHz)	$I_A(t, t)$ (dBm)
$l_1 = 1310$ nm	0	0	-14.68	-20.88	0.163	0	-27.986
$l_2 = 1550$ nm	0	0	-14.68	-20.88	0.163	0	-27.986

Table (10) Beat Signal at 1310 nm

1. $l_1 = 1310$ nm			
No.	Z (km)	$f_b$ (MHz)	I(t,t) (dBm)
1	0	0	$I_A = -27.986$
2	0.96	0.4	$I_B = -63.01$
3	5	2.08	$I_{C1} = -67.126$ $I_{C2} = -68.3$
4	10	4.16	$I_{D1} = -52.9$ $I_{D2} = -72.3$ $I_{D3} = -74.76$
5	15	6.24	$I_{E1} = -80.04$ $I_{E2} = -81.2$
6	20	8.34	$I_{F1} = -51.25$ $I_{F2} = -85.325$ $I_{F3} = -116.99$

Table (11) Beat Signal at 1550 nm

2. $l_2 = 1550$ nm			
No.	Z (km)	$f_b$ (MHz)	I(t, t) (dBm)
1	0	0	$I_A = -27.986$
2	0.96	0.4	$I_B = -63.01$
3	5	2.08	$I_{C1} = -68.013$ $I_{C2} = -69.5$
4	10	2.08	$I_{D1} = -52.038$ $I_{D2} = -72.65$ $I_{D3} = -75.153$
5	15	6.24	$I_{E1} = -79.547$ $I_{E2} = -87.852$
6	20	8.34	$I_{F1} = -56.533$ $I_{F2} = -92.248$ $I_{F3} = -116.99$

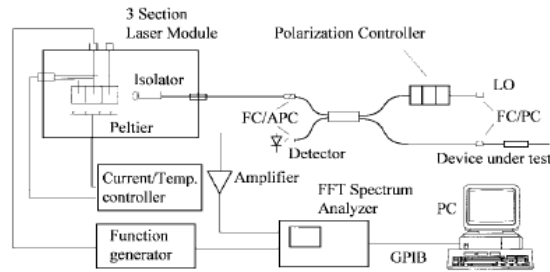


Figure (1) Block diagram for OFDR Measurements[3]

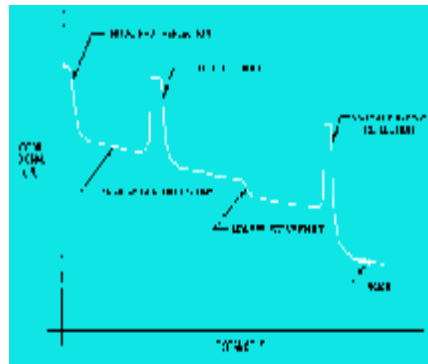


Figure (2) Types of faults of optical fiber[5]

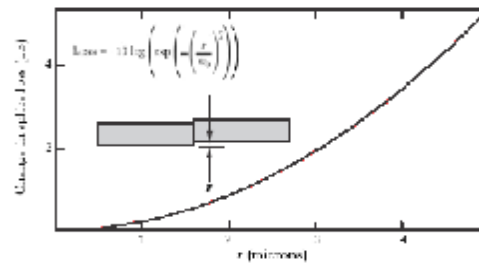


Figure (3) Coupling loss in single-mode fiber as a function of lateral misalignment[8].

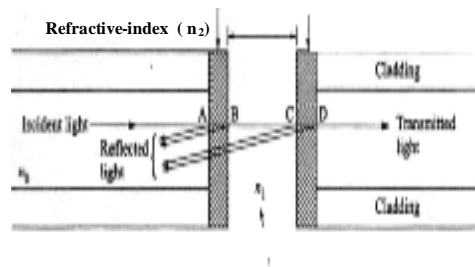
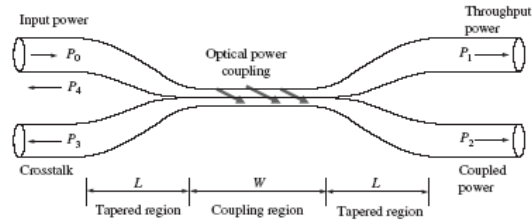
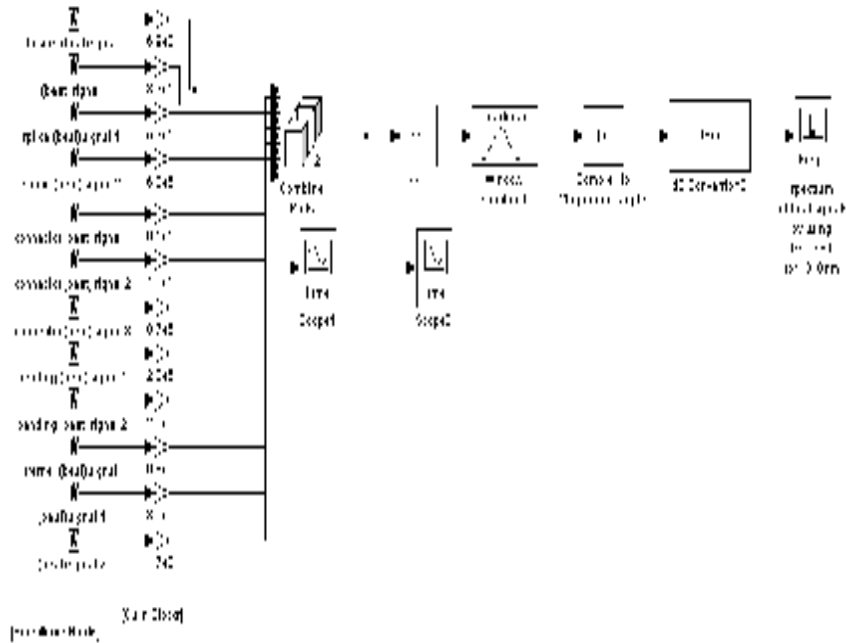


Figure (4) model of an index-matched connection with perpendicular fiber end face [9]



**Figure (5) Cross-sectional view of a fused-fiber coupler having a coupling region  $W$  and two tapered regions of length  $L$ . The total span  $(2L + W)$  is the coupler draw length[11].**



**Figure (6) Design model for all Faults detection**

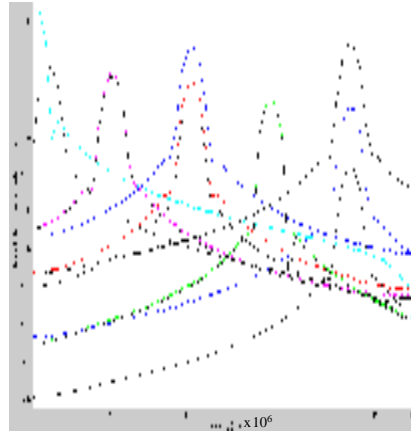


Figure (7) : Beat signals of defect optical fiber by using (OFDR) at wavelength (1310nm) by (DFT-FFT) ) :1) Fresnel reflection fault.2)splice fault. 3) connector fault.4) bending fault .

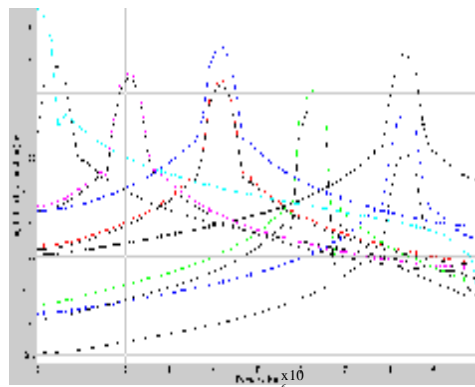


Figure (8) : Beat signals of defect optical fiber by using (OFDR) at wavelength (1550nm) by (DFT-FFT) ) :1)Fresnel reflection fault.2)splice fault. 3)connector fault.4) bending fault .

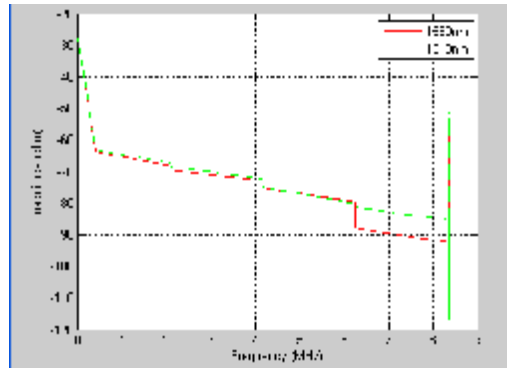


Figure (9) Beat signals of defect optical fiber by using (OFDR) at Wavelength (1310nm,1550nm) :1)Fresnel reflection fault.2)splice fault. 3) connector fault.4) bending fault .

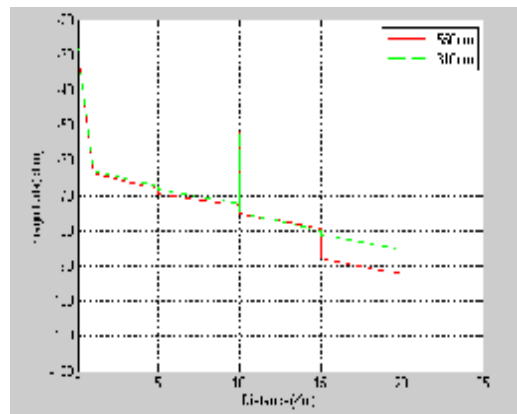


Figure (10) Beat signals of defect optical fiber by using (OFDR) at Wavelength (1310nm,1550nm) 1)Fresnel reflection fault.2)splice fault. 3) connector fault.4) bending fault

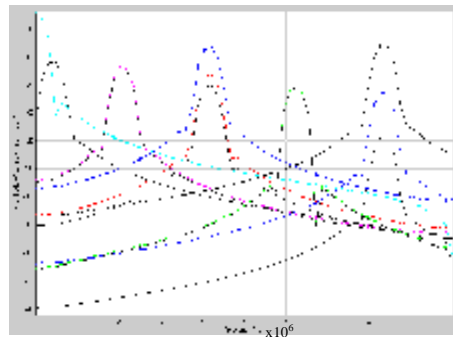


Figure (11) Reflected beat signals from SM defect optical fiber at (1310nm) for different faults

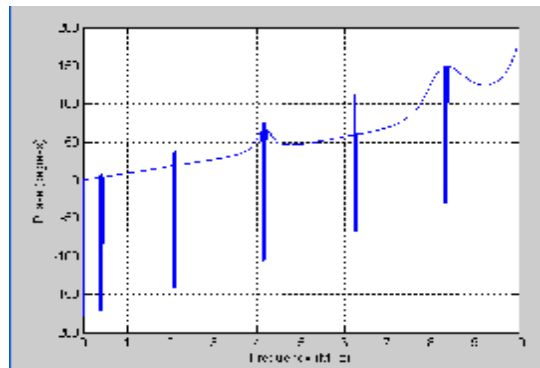


Figure (12) Faults detection by (PHASE) for defected SM optical fiber by using (OFDR) with (DFT-FFT) .

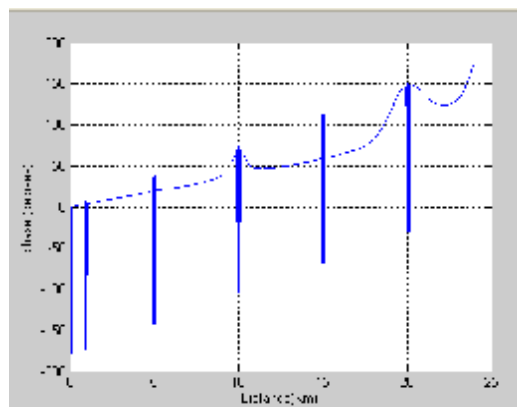


Figure (13) :Faults detection by (PHASE) for defected SM optical fiber by using (OFDR) with (DFT-FFT) .